

**UNSTEADY MAGNETOHYDRODYNAMIC FLUID
FLOW IN A COLLAPSIBLE TUBE**

KIGO JAMES MWANGI

MASTER OF SCIENCE

(Applied Mathematics)

**JOMO KENYATTA UNIVERSITY OF
AGRICULTURE AND TECHNOLOGY**

2016

Unsteady magnetohydrodynamic fluid flow in a collapsible tube

Kigo James Mwangi

A thesis submitted in partial fulfilment for the degree of Masters of
Science in Applied Mathematics in the Jomo Kenyatta University of
Agriculture and Technology

2016

DECLARATION

This thesis is my original work and has not been presented for a degree in any other University.

Signature.....Date.....

Kigo James Mwangi

This thesis has been submitted for examination with our approval as university Supervisors.

Signature.....Date.....

Prof. Mathew Ngugi Kinyanjui

JKUAT, KENYA

Signature.....Date.....

Dr. Kang’ethe Giterere

JKUAT, KENYA

DEDICATION

To my dad Mr. Daniel Kigo and my mum Mrs. Anne Kigo for their parental guidance and their enduring support towards my education and to my siblings Priscilla, John and Joyce for their encouragement.

ACKNOWLEDGEMENT

First and foremost, my appreciation goes to my supervisors Prof. Mathew N. Kinyanjui and Dr. Kang'ethe who have worked tirelessly to make this study a success. Their guidance and positive criticism have gone a long way in enhancing the quality of this study. The knowledge I have acquired from my supervisors will go a long way in helping me in my future research work and related fields which I intend to undertake especially in Applied Mathematics.

Secondly, and by no order of preference I thank Dr. Kiogora, Mr. Kihuga, Ms. Ndanu Mr. Njagi, Mr. Mburu, Mr. Karuiru, Mr. Makumi, Ms. Christine, Mr. Mark, Mr. Nyariki, and Mr. Muriuki for the contribution and encouragement they gave me.

Thirdly, much appreciation goes to the secretary PAM department Ms. Hellen, and Mathematics and Computer Laboratory Technical Staff for their technological assistance during the research period.

Above all I thank the Almighty for the great health, great opportunities and good mind set during the research period.

TABLE OF CONTENTSⁱ

DECLARATION	ii
DEDICATION	iii
ACKNOWLEDGEMENT	iv
NOMENCLATURE	viii
LIST OF FIGURES	xi
LIST OF ABBREVIATIONS	xii
ABSTRACT	xiii
CHAPTER ONE	1
1.0 Introduction	1
1.1 Definitions	3
1.1.0 Fluid	3
1.1.1 Viscosity	3
1.1.2 Collapsible tube	4
1.1.3 Compressible and incompressible fluids	4
1.1.4 Newtonian fluids.....	4
1.1.5 Non-Newtonian fluids.....	5
1.1.6 Unsteady and steady flow.	5
1.1.7 Magneto fluid dynamics	6
1.2 Literature Review	6
1.3 Statement of the Problem	12
1.4 Justification	12
1.5 Hypothesis	14
1.6 Objectives	14
1.6.1 General objective	14
1.6.2 Specific Objectives	14
CHAPTER TWO	15
MATHEMATICAL FORMULATION	15
2.1 Introduction	15
2.2 Assumptions	15
2.3 Governing Equations	15
2.3.1 Equation of continuity	15

2.3.2 Equation of conservation of momentum.....	16
2.3.3 Lorentz Force.....	18
2.3.4 Equation of energy.....	19
2.4 Non-Dimensional Numbers.....	22
2.4.1 Reynolds number.....	22
2.4.2 Prandtl Number Pr.....	22
2.4.3 Eckert Number.....	22
2.4.4 Hartmann Number.....	23
2.5 Nondimensionalisation.....	23
CHAPTER THREE.....	27
METHODOLOGY.....	27
3.1 Introduction.....	27
3.2 Finite Difference Method.....	27
3.3 The discrete mesh.....	28
3.3.1 Finite Difference Approximations.....	28
3.3.2 First Order Forward Finite Difference.....	29
3.3.3 First Order Finite Central Difference.....	31
3.3.4 Second Order Finite Central Difference.....	32
3.3.5 Crank-Nicholson method.....	33
3.4 Consistence, Convergence and Stability of a FDM.....	33
3.4.1 Consistency.....	33
3.4.2 Convergence.....	33
3.4.3 Stability.....	34
CHAPTER FOUR.....	37
RESULTS AND DISCUSSIONS.....	37
4.1 Introduction.....	37
4.2 Primary velocity profiles.....	37
4.3 Temperature profiles.....	42
4.4 Validation of Results.....	47
CHAPTER FIVE.....	48
CONCLUSIONS AND RECOMMENDATIONS.....	48
5.1 Introduction.....	48

5.2 Conclusions	48
5.3 Recommendations	49
REFERENCES	50
APPENDICES	52
COMPUTER CODE IN MATLAB.....	52
PUBLICATION	54

NOMENCLATURE

Roman Symbol	Quantity
B	Magnetic field strength vector, [Wbm^{-2}]
H_0	Magnetic flux identity, [Wbm^{-2}]
H	Magnetic field intensity vector, [Am^{-1}]
g	Acceleration due to gravity vector, [ms^{-2}]
J	Current density, [Am^{-2}]
E	Electric field, [v]
M	Magnetic parameter
Re	Reynolds number
P	Pressure force, [Nm^{-2}]
P^*	Dimensionless pressure force
q	Velocity vector, [ms^{-1}]
F_i	Body forces tensor, [N]
F_e	Electromagnetic force, [Kgms^{-2}]
Pr	Prandtl number
H	Hartman number

P	Internal pressure, [Pa]
P_E	External pressure, [Pa]
P_t	Transmural pressure ($P-P_E$), [Pa]
A	Cross sectional area, [m ²]
L	Peripheral length, [m]
∇^2	Laplacian Operator
r, θ, z	Cylindrical coordinates
t	Time, [s]
\mathbf{F}	Body force, [N]
T	Temperature, [K]
u^*, v^*	Dimensionless velocity
t^*	Dimensionless time
U_0	Characteristic velocity, [ms ⁻¹]
C_P	Specific heat at constant pressure, [JKg ⁻¹ K ⁻¹]
T_∞	Characteristic temperature, [K]

Greek symbol	quantity
ν	Kinematic viscosity of the fluid, [m ² s ⁻¹]
ρ	Fluid density, [kgm ⁻³]
μ	Coefficient of viscosity, [kgm ⁻¹ s ⁻¹]
σ	Electrical conductivity, [Ω^{-1} m ⁻¹]
κ	Thermal conductivity, [Wm ⁻¹ K ⁻¹]
ϕ	Viscous dissipation function, [s ⁻²]
$\Delta t, \Delta r, \Delta z$	Time and two distance intervals respectively, [s, m]
ΔT	Temperature change, [K]

LIST OF FIGURES

Figure 1.1: Geometry of the problem.....	12
Figure 3.1: Finite difference mesh	29
Figure 4.1: Velocity profiles for $M=4$, $P=-10$, $t=100$	38
Figure 4.2: Velocity profiles for $R=7.1$, $P=-10$, $t=100$	39
Figure 4.3: Velocity profiles for $R=7.1$, $M=4$, $P=-10$	40
Figure 4.4: Velocity profiles for $R=7.1$, $M=4$, $t=100$	4138
Figure 4.5: Temperature profiles for $H=4$, $Ec=0.5$, $t=100$	4339
Figure 4.6: Temperature profiles for $H=4$, $Pr=21$, $t=100$	4440
Figure 4.7: Temperature profiles for $Pr=21$, $Ec=0.5$, $t=100$	4641

LIST OF ABBREVIATIONS

FDM	Finite Difference Method
BFD	Biomagnetic Fluid Dynamics
MHD	Magnetohydrodynamics
MFD	Magnetofluidynamics
PDE's	Partial Differential Equations
MATLAB	Matrix Laboratory
HOT	Higher Order Terms

ABSTRACT

In this research, unsteady magnetohydrodynamic fluid flow in a collapsible tube has been investigated. The study is aimed at determining the velocity profiles, temperature profiles and the effects of varying dimensionless numbers on the flow variables. The tube is considered to be collapsible in the transverse direction, taken to be perpendicular to the main flow direction. The fixed magnetic field is perpendicular to the direction of flow of the conducting fluid. The equations governing the flow are non-linear and cannot be solved analytically. Therefore an approximate solution to the equations is determined numerically. In this case, finite difference method is used. A computer program is then used to generate results which are presented in form of graphs. The results on varying various non-dimensional parameters on temperature and velocity profiles are then discussed. It is noted that a change in the value of dimensionless parameters leads to either increase, decrease or to have no effect on velocity and Temperature profiles respectively. The results obtained can be applied in medical field and also in industries where collapsible tubes are used.

CHAPTER ONE

1.0 Introduction

Hydrodynamics is the science that is concerned with the flow of fluids and Magneto hydrodynamics is the study of motion of electrically conducting fluid in presence of magnetic field. The flow of an electrically conducting fluid under a magnetic field gives rise to an induced electric current. The induced electric current also produces induced magnetic field thus the original magnetic field is changed. The two way interaction between the flow field and the magnetic field exerts a force on the fluid particles. Thus the hydromagnetic flows are more complex than the ordinary hydrodynamic flows.

A tube with a circular cross-section is said to be collapsible if the tube has sufficiently flexible walls such that it can elastically accommodate deformation when there is a difference between the magnitudes of the external pressure and internal pressure. When fluid flows through the collapsible tube, various phenomena are revealed. Such phenomena occur rarely in industrial applications but are very common in biological studies such as blood flow in veins and air flow in lungs. Collapsing occurs in the veins such as veins of a hand raised above the level of the heart or in the jugular vein when a person is standing upright. In the arteries, collapse occurs when high external pressures are applied, such as when an artery is compressed by a sphygmomanometer cuff during blood pressure measurement. Similarly, in the industry collapse may be experienced during cementing operations, trapped fluid expansion, or well evacuation, among many others. Most oilfield tubulars also experience collapse.

Blood is essential in sustaining life as it transports oxygen and nutrients to all parts of the body, relays chemical signals and moves metabolic waste to the kidneys for elimination. A quantitative model of blood flow is important not only as it relates to clinical diagnosis of disease, but as an integral component of models of more complex structures. To date, numerous mathematical models have been developed to describe blood flow in the circulatory system. Following such a tradition but looking at different aspect, this thesis adopts the biomagnetic fluid model in representing the blood flow. A biomagnetic fluid is defined as a fluid that exists in a living creature and its flow is influenced by the presence of a magnetic field. Due to the complex interaction of the intercellular protein, cell membrane and the hemoglobin, a form of iron oxides presents at a uniquely high concentration in the mature red blood cells (erythrocytes). Its magnetic property is affected by factors such as the state of oxygenation. Research has been done on the fluid dynamics of biological fluids in the presence of magnetic field and useful applications have been proposed in bioengineering and medicine. Among them are the developments of magnetic devices for cell separation, targeted transport of drugs i.e. using magnetic particles as drug carriers, magnetic wound treatment and cancer tumor treatment, reduction of bleeding during surgeries and provocation of occlusion of the feeding vessels of cancer tumors and development of magnetic tracers.

It is imperative to acknowledge that mathematical modeling and numerical simulations provide many important insights on the underlying interactions between blood flow and magnetic field, some of which are not directly assessible through experimental investigation. Computational simulations make possible the study of

the feasibility of a medical technique before entering clinical trials, and simulations are useful for investigating the influence of various factors independently.

1.1 Definitions

In this study several terms have been used extensively and such terms are defined in this section.

1.1.0 Fluid

A fluid is a substance that continually deforms under an applied shear stress. Fluids are a subset of the phases of matter and include liquids, gases, plasmas and to some extent plastic solids. Fluids can be defined as substances that have zero shear modulus or in simpler terms a fluid is a substance which cannot resist any shear force applied to it.

1.1.1 Viscosity

This is the resistance set up due to shear stresses within the fluid particles and the shear stresses between the fluid particles and the solid surface for a fluid flowing around a solid body. As fluid exerts a shear stress on the boundary, the boundary exerts an equal and opposite force on the fluid called shear resistance (frictional drag). Drag coefficient always depends on the Reynolds number (Re) and the shape of the body. The work done against the viscous effects usually causes fluid flow, consequently the energy spent in doing so is converted to heat. At low values of Reynolds number, the fluid is highly viscous causing deformation drag, the fluid is deformed in a wide zone around the body which brings about pressure force and frictional force. At large values of Reynolds number, the fluid is less viscous for example in water and air, the viscous effect is limited to the boundary layer

thickness. In this case deformation drag is exclusively friction drag. The shear force exerted on the surface of the body due to the formation of boundary layer results into friction drag.

1.1.2 Collapsible tube

A tube with a circular cross-section is said to be collapsible if the tube has sufficiently flexible walls such that it can elastically accommodate deformation when there is a difference between the magnitudes of the external pressure and internal pressure.

1.1.3 Compressible and incompressible fluids

A fluid is said to be compressible if its density changes appreciably within the domain of interest. Typically, this will occur when the fluid velocity exceeds Mach 0.3. Hence, low velocity fluid flows behave as incompressible. An incompressible fluid is one whose density is constant. In many practical cases of fluid flow, the variation of density of the fluid may be neglected. This is particularly important when the fluid flow is due to buoyant forces and in such cases, the fluid is considered to be incompressible.

1.1.4 Newtonian fluids

In a Newtonian fluid, the relation between the shear stress and the strain rate is linear (and if one were to plot this relationship, the line would pass through the origin), the constant of proportionality being the coefficient of viscosity. For a Newtonian fluid, the viscosity, by definition, depends only on temperature, pressure and the chemical composition of the fluid, not on the forces acting upon it. In common terms, this means the fluid continues to flow, regardless of the forces acting on it. For example,

water is Newtonian, because it continues to exemplify fluid properties no matter how fast it is stirred or mixed.

1.1.5 Non-Newtonian fluids

In a non-Newtonian fluid, the relation between the shear stress and the strain rate is nonlinear, and can even be time-dependent. Therefore a constant coefficient of viscosity cannot be defined.

A non-Newtonian fluid is a fluid whose flow properties are not described by a single constant value of viscosity. Many polymer solutions and molten polymers are non-Newtonian fluids, as are many commonly found substances such as starch suspensions, paint and blood.

1.1.6 Unsteady and steady flow.

For steady flow the velocity at any given point in space does not vary with time, i.e.

$\frac{\partial \mathbf{q}}{\partial t} = 0$. In reality almost all flows are unsteady in some sense, that is, the velocity

varies with time. An example of a non-periodic, unsteady flow is that produced by turning off a faucet to stop the flow of water. In other flows the unsteady effects may be periodic, occurring time after time in basically the same manner. The periodic injection of the air-gasoline mixture into the cylinder of an automobile engine is such an example. In many situations the unsteady character of a flow is quite random, that is, there is no repeated regular variation to the unsteadiness. This behavior occurs in turbulent flow and is absent in laminar flow. The “smooth” flow of highly viscous syrup onto a pancake represents a “deterministic” laminar flow. It is quite different from the turbulent flow observed in the “irregular” splashing of water from a faucet onto the sink below it. The “irregular” gustiness of the wind represents another

random turbulent flow. In an unsteady flow, the flow variables such as velocity and the thermodynamic properties at every point in space vary with respect to time.

1.1.7 Magneto fluid dynamics

Faraday's law of electromagnetic induction reveals that when a conductor is moving across a magnetic field, an electromotive force is produced in the conductor. Also, when a current carrying conductor is moving in a magnetic field it experiences a force that tends to move it at right angles to the electric field. Lenz's law gives the direction of the induced current as that direction that opposes the change in the magnetic field that causes it. When an electrically conducting fluid moves past a magnetic field, there arises an interaction between the flow field and the magnetic field. The magnetic field exerts a force on the fluid due to induced currents and the induced currents affect the original magnetic field. If these electromagnetic forces generated are of the same order of magnitude as the hydrodynamic forces then these electromagnetic forces have to be taken into account when considering the flow field. MFD fluid flows involve the flow of electrically conducting fluids in the presence of a magnetic field. MFD therefore is a field of study involving both electromagnetic theory and fluid dynamics.

1.2 Literature Review

Flow through collapsible tubes has been extensively studied in the laboratory. In experimental studies flexible tubing is employed. According to Edward, (1972) these experiments are based upon the assumption that the difference between the flexible tubing and veins are quantitative in nature rather than qualitative.

Bertram, (1986). did an experimental study on collapsible and elastic tubes and observed that when the external pressure exceeded the internal fluid pressure the tube buckled non-axisymmetrically, leading to a nonlinear relation between pressure-drop and flow rate. Bertram *et al.* (1990). explained that at sufficiently large Reynolds numbers, the system produces self-excited oscillations, and exhibits hysteresis in transitions between dynamical states, multiple modes of oscillations (each having distinct frequency range), rich and complex nonlinear dynamics.

Mawasha et al. (2001). investigated the dynamic behavior of a collapsible tube system consisting of a reservoir with inlet and outlet flow conditions using a nonlinear analysis approach. The reservoir was subjected to a constant inlet flow rate and the outlet flow rate and the pressure–flow rate relation of the downstream collapsible regime was presented by a constitutive model containing a cubic nonlinearity. The relaxation oscillations observed for collapsible tube model were analogous to the behavior of the van der pol oscillator. The van der Pol oscillator is a canonical model for self-excited nonlinear oscillations exhibited in electrical circuits.

Andrew, (2003) investigated the steady flow of a viscous fluid through a thin-walled elastic tube mounted between two rigid tubes. The steady three-dimensional Navier–Stokes equations were solved simultaneously with the equations of geometrically nonlinear Kirchhoff–Love shell theory. He explained that if the transmural (internal minus external) pressure acting on the tube is sufficiently negative then the tube buckles non-axisymmetrically and the subsequent large deformations leads to a strong interaction between the fluid and solid mechanics. The main effect of fluid inertia on the macroscopic behavior of the system is due to the Bernoulli effect,

which induced an additional local pressure drop when the tube buckles and its cross-sectional area is reduced. Thus, the tube collapses more strongly than it would in the absence of fluid inertia.

Brian, (2003) formulated a mathematical model for a collapsible tube and developed a computational methodology to determine the best-fit values for parameters that describe constitutive behavior of the tube. He noted that the tube stiffness affected the cross sectional area of the tube and had no large influence on the internal pressure.

Heil et al. (2003) explained that nonaxisymmetrically collapsed vessels readily develop flow-induced, self excited oscillations. Hazel et al. (2003) investigated the steady flow through thin-walled elastic tubes for a finite Reynolds number. Results indicated that non axisymmetric buckling of the tube contributes to nonlinear pressure-flow relations that can exhibit flow limitation through purely viscous mechanisms.

Makinde, (2005) described the fluid dynamics of a collapsible tube using a mathematical model. He noted that fluid axial velocity generally decreases with an increase in tube contraction due to the strong influence of the negative transmural pressure owing to marked reduction of rigidity.

Prashanta, (2005) studied the problem of non-Newtonian and non-linear blood flow through a stenosed artery. Finite difference scheme was used to solve the unsteady nonlinear Navier-stokes equations in cylindrical coordinates assuming axial symmetry under laminar flow condition. The model was also employed to study the

effects of the taper angle, wall deformation, severity of the stenosis within its fixed length, steeper stenosis of the same severity, nonlinearity and non-Newtonian rheology of the flowing blood on the flow field. Quantitative analysis was performed through numerical computations. He concluded that that the axial velocity profile assumed a flat shape in the presence of a converging tapering instead of a parabolic one for non-tapered artery when both are treated under stenotic conditions. He explained that if the tube is tapered, then inertial forces associated with the convective accelerations manifest themselves in an amount of the same order as viscous forces while the former compel the axial velocity profile to attain a flat shape.

Marzo *et al.* (2005) studied three-dimensional collapse of a steady flow through finite-length elastic tubes numerically. Odejide *et al.* (2008) examined an incompressible viscous fluid flow and heat transfer in a collapsible tube. It was also noted that increase in Reynolds number led to an increase in the fluid temperature with maximum magnitude at the pipe center and minimum at the wall. The fluid velocity profile was noted to be parabolic in nature.

Andrew *et al.* (2008) described the role of venous valves in pressure shielding. A one-dimensional mathematical model of a collapsible tube with the facility to introduce valves at any position was used. They observed that a valve decreased the dynamic pressures applied to a vein when gravity is applied by a considerable amount.

Liu *et al.* (2009) explained that the wall stiffness is dominated by the axial tension. Eleuterio, (2013) formulated a one-dimensional time-dependent non-linear

mathematical model for physiological fluid flow in collapsible tubes with discontinuous material properties. He observed that although the solution algorithm dealt with idealized cases, it is uniquely well-suited for assessing the performance of numerical methods intended for simulating more general situations.

Emilie *et al.* (2010) developed a simple and effective numerical physiological tool to help clinicians and researchers in the understanding of flow phenomena. One-dimensional Runge–Kutta discontinuous Galerkin (RK-DG) method coupled with lumped parameter models for the boundary conditions was used. Various benchmark problems that showed the flexibility and applicability of the numerical method were presented. The emptying process in a calf vein squeezed by contracting skeletal muscle in a normal and pathological subject was also studied and the results compared with experimental simulations. After the comparison of the results it was noted that the efficiency of muscular calf pump is strongly dependent on the valves pathology and the walking frequency.

Annunziato *et al.* (2013) formulated a one-dimensional time-dependent non-linear mathematical model for physiological fluid flow in collapsible tubes with discontinuous material properties, i.e. vessel wall thickness, equilibrium cross sectional area and Young's modulus. In particular, a mathematical model for blood flow in medium to large arteries and veins was studied. The resulting hyperbolic system was analysed and the associated Riemann problem solved exactly. They explained that although the solution algorithm dealt with idealised cases, it is uniquely well-suited for assessing the performance of numerical methods intended for simulating more general situations.

Siviglia *et al.* (2013) performed a steady analysis of transcritical flows in collapsible tubes with discontinuous mechanical properties. They found transcritical curves that describe the conditions under which the incoming flow inside a collapsible tube may pass through the critical state due to an abrupt change of the mechanical properties of the wall vessel. They investigated two different cases. In the first case they assumed a simplified tube law i.e $\beta_2 = 0$ and in the second they considered a complete tube law (i.e. $\beta_1 \geq 0$ and $0 < \beta_2 \leq 2$). For both cases they described the full range of conditions for which transition can occur. In particular they identified the values of the speed indexes, one supercritical and one subcritical, which are the limits of the transcritical region, and the associated values of the area ratio α which are related to the values of the transmural pressure.

Kanyiri *et al.* (2014) studied the effects of flow parameters (tube stiffness and longitudinal tension) on the flow variables of a Newtonian fluid flowing through a cylindrical collapsible tube. The results show that the flow parameters considered are directly proportional to both the cross sectional area and internal pressure and inversely proportional to the flow velocity.

Boileau *et al.* (2015) modeled the numerical schemes for one-dimensional arterial blood flow. They showed that arterial pulse wave haemodynamics can be accurately simulated using finite element, finite volume or finite difference methods.

Extensive research work has been done, including those cited above, on fluid flow in collapsible tubes. However, no emphasis has been given in consideration of magnetic field. The aim of this work is therefore to study unsteady magnetohydrodynamic fluid flow in a collapsible tube.

1.3 Statement of the Problem

This study has considered the analysis of unsteady magnetohydrodynamic fluid flow in a collapsible tube. The tube is cylindrical whereby the z axis lies along the center of the collapsible tube, $r = a_0(1 - \alpha t)^{\frac{1}{2}}$ is the distance measured radially, u and v are velocity components in the directions of z and r respectively and B_0 is the Magnetic field strength. A sketch diagram of the research problem is as shown in figure below.

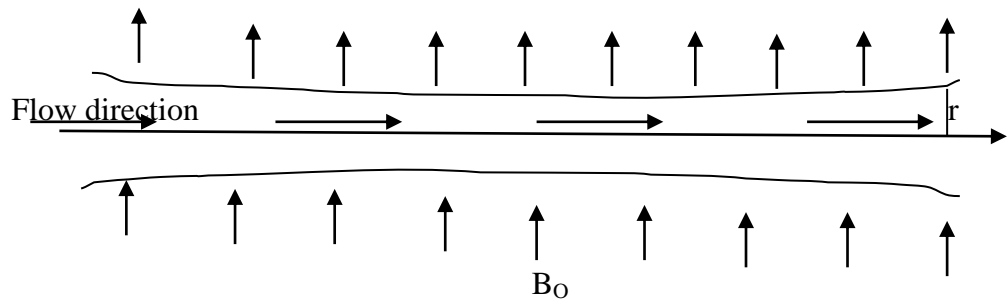


Figure 1.1: Geometry of the problem

1.4 Justification

The study of flow through collapsible tubes is of utmost importance in biological studies as well as in industries. Biomagnetic fluid dynamics is a relatively new area in fluid mechanics investigating the fluid dynamics of biological fluids in the presence of magnetic field. The study of biomagnetic fluid dynamics has applications in bioengineering and medical sciences. Among them is the development of magnetic devices for cell separation, targeted transport of drugs using magnetic

particles as drug carriers, magnetic wound or cancer tumor treatment causing magnetic hyperthermia, reduction of bleeding during surgeries or provocation of occlusion of the feeding vessels of cancer tumors and development of magnetic tracers.

This research is a useful input in medicine in understanding the behavior and analysis of flow phenomenon in veins, arteries, airways, urethra, etc. The study of flow through collapsible tubes is very useful in studying and predicting many diseases, such as the lung disease (asthma and emphysema), or the cardiovascular diseases (heart stroke).

Magnetic therapy for healing has been around for centuries. Many ancient civilizations used magnets for medical purposes. Recently the use of magnets has come back into medical use. It is theorized that magnets attract metal elements in the body, such as iron in blood, to increase blood circulation and therefore instigate healing. The increase in blood flow from magnets delivers more oxygen and natural painkillers called endorphins, which in turn relieves minor pain.

In addition to relieving pain, magnets can reduce inflammation with the increased blood circulation. When inflammation decreases, the patient can also heal more quickly.

Magnets can also attract the positive charges of various toxins formed by the body's immune system when fighting infection. The increased blood flow will then transports the toxins to the liver for speedy detoxification and eventual elimination from the body through the kidneys.

1.5 Hypothesis

Magnetic fields have no effect on velocity and temperature profiles of the fluid flow through collapsible tube.

1.6 Objectives

1.6.1 General objective

To investigate unsteady magneto hydrodynamic fluid flow in a collapsible tube.

1.6.2 Specific Objectives

- i. To determine the velocity profiles of the flow.
- ii. To determine the temperature profiles of the flow.
- iii. To determine the effects of varying dimensionless numbers on the flow variables.

In the next chapter, the general equations governing the flow through a collapsible tube are discussed. The assumptions taken into consideration are outlined and the governing equations are formulated. The method of solving these governing equations has also been discussed.

CHAPTER TWO

MATHEMATICAL FORMULATION

2.1 Introduction

In this chapter the equations governing the flow through a collapsible tube are given. This chapter starts by stating some of the assumptions taken into consideration and then formulating the governing equations for this flow.

2.2 Assumptions

1. The velocity of the fluid is very small compared to that of light.
2. The flow is unsteady.
3. The flow is laminar.
4. Electrical conductivity and thermal conductivity are constant.
5. The force due to electric field is negligible compared with Lorenz force due to magnetic field.
6. The induced magnetic field, the external electric field and the electric field due to the polarization of charges are negligible.
7. Flow separation occurring in a collapsed region of the tube is not a significant phenomenon
8. Tensile force throughout the collapsible tube is constant.

2.3 Governing Equations

Under the above assumptions, the governing equations are:

2.3.1 Equation of continuity

The equation of continuity also known as the equation of conservation of mass is quoted based on two fundamental principles namely:

- i. The mass of fluid is conserved i.e. the fluid is neither created nor destroyed in the field of flow.
- ii. The flow is continuous i.e. empty spaces do not occur between particles which were in contact

The general continuity equation is given by;

$$\frac{\partial \rho}{\partial t} + \nabla(\rho \mathbf{q}) = 0 \quad (2.1)$$

In this study we are considering an incompressible fluid i.e. the density is assumed to be constant. Thus equation (2.1) reduces to

$$\nabla \mathbf{q} = 0 \quad (2.2)$$

In polar form a two dimensional fluid flow equation is expressed as

$$\frac{\partial \mathbf{u}}{\partial z} + \frac{1}{r} \frac{\partial(r\mathbf{v})}{\partial r} = 0 \quad (2.3)$$

Considering the velocity in radial distance to be negligible

$$\frac{\partial \mathbf{u}}{\partial z} = 0 \quad \text{the equation reduces to} \quad (2.4)$$

2.3.2 Equation of conservation of momentum

The principle of conservation of momentum is basically an application of Newton's second law of motion to an element of fluid motion. Newton's second law of motion states that the rate of change of momentum of a body is equal to the net sum of resultant forces acting on the body. In this case, the body in consideration is the fluid. For a fluid in motion, some forces act within the fluid itself while other forces act on the fluid from external sources. Forces acting at a distance on a fluid particle are

referred to as body forces while surface forces refer to the forces due to direct contact of a fluid with other fluid particles or solid walls.

In the equation of momentum, the rate of change of momentum balance with the body forces and the surface forces. Body forces are forces that are proportional to the volume element and act on the fluid element from external force field e.g. gravitational force and centrifugal force while surface forces are proportional to area and they result from stresses such as static pressure and viscous stresses acting on the surface of the volume element. The forces acting on the fluid have to be specified for a particular flow configuration being considered.

The general equation of motion is written as;

$$\rho \left(\frac{\partial u_i}{\partial t} + u_i \frac{\partial u_i}{\partial x_i} \right) = - \frac{\partial p}{\partial x_i} + \mu \frac{\partial^2 u_i}{\partial x_i^2} + \rho \bar{F}_i \quad (2.5)$$

From equation(2.5) the terms $\frac{\partial u_i}{\partial t}$ and $u_i \frac{\partial u_i}{\partial x_i}$ represent the local and convective acceleration respectively and \bar{F}_i represent the body forces acting on the fluid.

The momentum equation in cylindrical coordinates for a two dimensional flow is given as

$$\frac{\partial u}{\partial t} + u \frac{\partial u}{\partial z} + v \frac{\partial u}{\partial r} = - \frac{1}{\rho} \frac{\partial p}{\partial z} + \frac{\mu}{\rho} \left(\frac{\partial^2 u}{\partial z^2} + \frac{1}{r} \frac{\partial u}{\partial r} + \frac{\partial^2 u}{\partial r^2} \right) + F \quad (2.6)$$

In this study, body forces considered are electromagnetic force and gravitational force thus

$$\mathbf{F} = \mathbf{g} + \mathbf{J} \times \mathbf{B} \quad (2.7)$$

By the assumption that the tube is horizontal the only body force to be considered is the electromagnetic force.

$$\text{Hence } \mathbf{F} = \mathbf{J} \times \mathbf{B} \quad (2.8)$$

2.3.3 Lorentz Force

From the geometry of the flow the constant magnetic field \mathbf{B}_0 is applied in the direction perpendicular to that of fluid flow. The assumption that the induced magnetic field is negligible is made since Magnetic Reynolds number is very small for partially ionized fluid.

The generalized Ohm's law, neglecting Hall Effect, is expressed as

$$\vec{\mathbf{J}} = \sigma(\vec{\mathbf{E}} + \vec{\mathbf{q}} \times \vec{\mathbf{B}}) \quad (2.9)$$

The term $\vec{\mathbf{q}} \times \vec{\mathbf{B}}$ in equation (2.9) yields

$$\vec{\mathbf{q}} \times \vec{\mathbf{B}} = \begin{vmatrix} \hat{\mathbf{r}} & \hat{\boldsymbol{\theta}} & \hat{\mathbf{z}} \\ v & 0 & u \\ B_0 & 0 & 0 \end{vmatrix} = uB_0\hat{\boldsymbol{\theta}} \quad (2.10)$$

Assuming that $\vec{\mathbf{E}}$ is negligible the Ohm's law reduces to

$$\vec{\mathbf{J}} = \sigma u B_0 \hat{\boldsymbol{\theta}} \quad (2.11)$$

$$\text{Hence } \mathbf{J} \times \mathbf{B} = \begin{vmatrix} \hat{\mathbf{r}} & \hat{\boldsymbol{\theta}} & \hat{\mathbf{z}} \\ 0 & \sigma u B_0 & 0 \\ B_0 & 0 & 0 \end{vmatrix} = -\sigma B_0^2 u \hat{\mathbf{z}} \quad (2.12)$$

Therefore substituting equations (2.4), (2.8),(2.12) and the assumption that the fluid velocity in radial direction is negligible the momentum equation(2.6) in z direction reduces to

$$\frac{\partial u}{\partial t} = -\frac{1}{\rho} \frac{\partial p}{\partial z} + \nu \left(\frac{\partial^2 u}{\partial r^2} + \frac{1}{r} \frac{\partial u}{\partial r} \right) - \frac{\sigma u B_0^2}{\rho} \quad (2.13)$$

2.3.4 Equation of energy

The equation of conservation of energy is derived from the First Law of Thermodynamics, which states that energy is conserved in any process involving a thermodynamic system and its surroundings. It simply states that the increase in the internal energy of a system is equal to the amount of energy added by heating the system minus the amount lost as a result of the work done by the system on its surroundings. i.e.

$$dE = dQ - dW = dQ - Pdv \quad (2.14)$$

$$\text{Since } dW = pdv \quad (2.15)$$

For the flow of an incompressible fluid with constant fluid conductivity k , the energy equation is given by

$$\rho C_p \frac{DT}{Dt} = k \nabla^2 T + \mu \phi \quad (2.16)$$

Where $\mu \phi$ is the internal heating due to viscous dissipation, T is the absolute temperature of the fluid and $\frac{D}{Dt}$ is the material derivative. For an incompressible two-dimensional fluid flow

$$\phi = 2 \left[\left(\frac{\partial u}{\partial z} \right)^2 + \left(\frac{\partial v}{\partial r} \right)^2 \right] + \left(\frac{\partial u}{\partial r} + \frac{\partial v}{\partial z} \right)^2 \quad (2.17)$$

Equation (2.17) reduces to $\phi = \left(\frac{\partial u}{\partial r} \right)^2$, this is because longitudinal length $L \gg r$

hence $\frac{\partial u}{\partial z} = 0$ and the value of v equals zero since flow of the fluid in radial direction is negligible.

Considering ohmic heating due to electrical resistance of the fluid equation (2.16) becomes

$$\rho C_p \left(\frac{\partial T}{\partial t} + u \frac{\partial T}{\partial z} + v \frac{\partial T}{\partial r} \right) = k \left(\frac{\partial^2 T}{\partial r^2} + \frac{1}{r} \frac{\partial T}{\partial r} + \frac{\partial^2 T}{\partial z^2} \right) + \mu \left(\frac{\partial u}{\partial r} \right)^2 + \frac{J^2}{\sigma} \quad (2.18)$$

Simplifying the term inside the brackets on the left hand side of this equation (2.18) yields

$$u \frac{\partial T}{\partial z} + v \frac{\partial T}{\partial r} = 0 \text{ Since } \frac{\partial T}{\partial z} = 0 \text{ and } v = 0. \text{ Also the first term inside the brackets on}$$

the right hand side simplifies to $\frac{\partial^2 T}{\partial r^2} + \frac{1}{r} \frac{\partial T}{\partial r}$ since $\frac{\partial^2 T}{\partial z^2} = 0$

Therefore equation (2.18) becomes

$$\rho C_p \frac{\partial T}{\partial t} = k \left(\frac{\partial^2 T}{\partial r^2} + \frac{1}{r} \frac{\partial T}{\partial r} \right) + \mu \left(\frac{\partial u}{\partial r} \right)^2 + \frac{J^2}{\sigma} \quad (2.19)$$

$$\text{From equation (2.11) } \vec{J} = \sigma u B_0 \hat{\theta}, \text{ therefore } \frac{J^2}{\sigma} = \sigma u^2 B_0^2 \quad (2.20)$$

The energy equation (2.19) becomes

$$\rho C_p \frac{\partial T}{\partial t} = k \left(\frac{\partial^2 T}{\partial r^2} + \frac{1}{r} \frac{\partial T}{\partial r} \right) + \mu \left(\frac{\partial u}{\partial r} \right)^2 + \sigma u^2 B_0^2 \quad (2.21)$$

The appropriate boundary conditions are:

The axial velocity and temperature at the wall are prescribed as:

$$u = 0 \quad T = 0 \quad \text{For } r = 1$$

Regularity of solution along z-axis i.e. at the center of the tube.

$$u = u_0 \quad T = T_0 \quad \text{For } r = 0$$

2.4 Non-Dimensional Numbers

2.4.1 Reynolds number

The Reynolds number is important in analyzing any type of flow when there is substantial velocity gradient shear. The Reynolds number indicates the relative significance of the viscous effects compared to the inertia effect. The Reynolds number is equal to inertial force divided by the

$$\text{Re} = \frac{\rho U_0 L_0}{\mu} = \frac{U_0 L_0}{\nu} \quad \text{viscous force. It is expressed as;}$$

If the Reynolds number of the system is small, the viscous force is predominant and the effect of viscosity is important in the whole flow field. If Reynolds number is large, the inertia force is predominant and the effect of viscosity is important only in thin layer of the region near solid boundary.

2.4.2 Prandtl Number Pr

Prandtl Number is a dimensionless number approximating the ratio of momentum diffusivity and thermal diffusivity k . Pr thus provides a measure of relative effectiveness of momentum and energy transport by diffusion in the velocity and thermal boundary layers respectively.

$$\text{Pr} = \frac{\nu \rho C_p}{\kappa} = \frac{\mu C_p}{\kappa}$$

2.4.3 Eckert Number

This is a measure of kinetic energy of the flow relative to the enthalpy differences across the boundary layer.

$$Ec = \frac{u_0^2}{C_p(T_w - T_\infty)}$$

2.4.4 Hartmann Number

It is the ratio of the magnetic force to viscous force and is defined as;

$$H = \frac{\sigma \mu_e^2 B_0^2 \nu}{U^2}$$

2.5 Nondimensionalisation

The MHD equations are expressed in dimensionless form so that the relative strengths of the different terms in the fluid flow equations can be inferred by the size of any multiplying factors. The non-dimensionalization of the equations is performed by first selecting certain characteristic quantities, the variables may be non-dimensionalized according to the transformations below.

For this particular problem we let L , V , P and T to be the characteristic length, velocity, pressure and temperature respectively. To non-dimensionalise the equations governing the flow we used the transformations:

$$u^* = \frac{u}{u_0}, r^* = \frac{r}{a_0}, t^* = \frac{u_0 t}{a_0}, z^* = \frac{z}{a_0}, P^* = \frac{P}{\rho u_0^2}, T^* = \frac{T - T_\infty}{T_w - T_\infty} \quad (2.22)$$

In order to transform the equations of continuity, momentum, energy, and concentration into their respective non-dimensional form, the following analysis is first carried out:

$$\frac{\partial u}{\partial t} = \frac{\partial u}{\partial u^*} \frac{\partial u^*}{\partial t^*} \frac{\partial t^*}{\partial t} = \frac{u_0^2}{a_0} \frac{\partial u^*}{\partial t^*} \quad (2.23)$$

$$\frac{\partial u}{\partial r} = \frac{\partial u}{\partial u^*} \frac{\partial u^*}{\partial r^*} \frac{\partial r^*}{\partial r} = \frac{u_0}{a_0} \frac{\partial u^*}{\partial r^*} \quad (2.24)$$

$$\frac{\partial^2 \mathbf{u}}{\partial r^2} = \frac{\partial}{\partial r^*} \left(\frac{\partial \mathbf{u}}{\partial r^*} \frac{\partial r^*}{\partial r} \right) \frac{\partial r^*}{\partial r} = \frac{u_0 \partial^2 \mathbf{u}^*}{a_0^2 \partial r^{2*}} \quad (2.25)$$

$$\frac{\partial P}{\partial z} = \frac{\partial P}{\partial P^*} \frac{\partial P^*}{\partial z^*} \frac{\partial z^*}{\partial z} = \frac{\rho u_0^2 \partial P^*}{L \partial z^*} \quad (2.26)$$

$$\frac{\partial T}{\partial r} = \frac{\partial T}{\partial T^*} \frac{\partial T^*}{\partial r^*} \frac{\partial r^*}{\partial r} = \frac{(T_w - T_\infty)}{a_0} \frac{\partial T^*}{\partial r^*} \quad (2.27)$$

$$\frac{\partial T}{\partial t} = \frac{\partial T}{\partial T^*} \frac{\partial T^*}{\partial t^*} \frac{\partial t^*}{\partial t} = \frac{(T_w - T_\infty) u_0}{a_0} \frac{\partial T^*}{\partial t^*} \quad (2.28)$$

$$\frac{\partial^2 T}{\partial r^2} = \frac{\partial}{\partial r^*} \left(\frac{\partial T}{\partial T^*} \frac{\partial T^*}{\partial r^*} \frac{\partial r^*}{\partial r} \right) \frac{\partial r^*}{\partial r} = \frac{\partial}{\partial r^*} \left(\frac{(T_w - T_\infty)}{a_0^2} \frac{\partial T^*}{\partial r^*} \right) = \frac{(T_w - T_\infty)}{a_0^2} \frac{\partial^2 T^*}{\partial r^{2*}} \quad (2.29)$$

$$\frac{u_0^2}{a_0} \frac{\partial \mathbf{u}}{\partial t} = -\frac{u_0^2}{a_0} \frac{\partial P}{\partial z} + \frac{\mu u_0}{\rho a_0^2} \left(\frac{\partial^2 \mathbf{u}}{\partial r^2} + \frac{1}{r} \frac{\partial \mathbf{u}}{\partial r} \right) - \frac{\sigma u_0 B_0^2 \mathbf{u}}{\rho} \quad (2.30)$$

Substituting equations (2.23) to (2.26) into equation (2.13) and dividing the resulting

terms by $\frac{u_0^2}{a_0}$, the equations of momentum becomes:

$$\frac{\partial \mathbf{u}}{\partial t} = -\frac{\partial P}{\partial z} + \frac{\mu}{\rho a_0 u_0} \left(\frac{\partial^2 \mathbf{u}}{\partial r^2} + \frac{1}{r} \frac{\partial \mathbf{u}}{\partial r} \right) - \frac{\sigma a_0 B_0^2 \mathbf{u}}{\rho u_0} \quad (2.31)$$

$$\text{Or } \frac{\partial \mathbf{u}}{\partial t} = -\frac{\partial P}{\partial z} + \frac{1}{\text{Re}} \left(\frac{\partial^2 \mathbf{u}}{\partial r^2} + \frac{1}{r} \frac{\partial \mathbf{u}}{\partial r} \right) - M \mathbf{u} \quad (2.32)$$

Where $M = \frac{\sigma a_0 B_0^2}{\rho u_0}$ is the Magnetic field parameter, $\text{Re} = \frac{a_0 u_0}{\nu}$ is the Reynolds

number, Similarly substituting equations (2.24) , (2.27),(2.28)and(2.29) into equation

(2.21) and dropping the *s and dividing each of the resulting terms by $\frac{(T_w - T_\infty)}{a_0^2}$,

equation (2.21) becomes

$$u_0 a_0 \frac{\partial T}{\partial t} = \frac{\kappa}{\rho C_p} \left(\frac{\partial^2 T}{\partial r^2} + \frac{\partial T}{\partial r} \right) + \frac{\mu u_0^2}{\rho C_p (T_w - T_\infty)} \left(\frac{\partial u}{\partial r} \right)^2 + \frac{\sigma a_0^2 u_0^2 B_0^2 u^2}{\rho C_p (T_w - T_\infty)} \quad (2.33)$$

Where the following non dimensional numbers arise:

$$\frac{1}{Pr} = \frac{\kappa}{\rho C_p} \text{ prandtl number, } Ec = \frac{u_0^2}{C_p (T_w - T_\infty)} \text{ Eckert number} \quad \text{and}$$

$$H = \frac{\sigma a_0^2 u_0^2 B_0^2}{\rho C_p} \text{ Hartmann number}$$

Equation (2.33) reduces to

$$\frac{u_0 a_0}{\mu} \frac{\partial T}{\partial t} = \frac{1}{\mu Pr} \left(\frac{\partial^2 T}{\partial r^2} + \frac{\partial T}{\partial r} \right) + \frac{Ec}{\rho} \left(\frac{\partial u}{\partial r} \right)^2 + \frac{Hu^2}{(T_w - T_\infty)} \quad (2.34)$$

The non-dimensional boundary conditions are: $u = 0, T = 0$ For $r = 1$ Where u is the axial velocity and T is the temperature at the wall. Considering the normal blood flow velocity and body temperature the boundary conditions at the center of the tube are:

$$u = 0.45, T = 37 \text{ For } r = 0$$

In the next chapter, the method of solution is discussed; expounding on its advantages of stability, consistency, convergence and accuracy. The governing equations discussed in chapter two above are presented in their finite difference form.

CHAPTER THREE

METHODOLOGY

3.1 Introduction

In this chapter, the method of solution is discussed and the governing equations are presented in their finite difference form. These equations are solved by computer program code which is run in MATLAB version 7.9.0.529(R2009b).

3.2 Finite Difference Method

The finite difference method is one of several techniques for obtaining numerical solutions to differential equations. In all numerical solutions the continuous partial differential equation is written in finite difference form. The numerical solution is known only at a finite number of points in the physical domain. The number of those points can be selected by the user of the numerical method. In general, increasing the number of points not only increases the resolution, but also the accuracy of the numerical solution. The finite difference equations result in a set of algebraic equations that are solved. The set of locations where the solution is computed is referred to as the mesh. These points are called nodes, and if one were to draw lines between adjacent nodes in the domain the resulting image would resemble a net or mesh. Two key parameters of the mesh are Δr , the local distance between adjacent points in space, and Δt , the local distance between adjacent time steps. For this case Δr and Δt are uniform throughout the mesh. The core idea of the finite-difference method is to replace continuous derivatives with difference formulas that involve only the discrete values associated with positions on the mesh. The finite-difference of a differential equation involves replacing all derivatives with finite differences.

3.3 The discrete mesh

The finite difference method gives an approximate solution for $\phi(x, t)$ at a finite set of x and t . For the codes developed the discrete x are uniformly spaced in the interval $0 \leq x \leq l$ such that

$$x_i = (i-1)\Delta x \quad , i = 1, 2, \dots, N$$

Where N is the total number of spatial nodes, including those on the boundary. Given l and N , the spacing between the x_i is computed with

$$\Delta x = \frac{l}{N-1}$$

Similarly, the discrete t are uniformly spaced in $0 \leq t \leq t_{\max}$

$$t_m = (m-1)\Delta t \quad , m = 1, 2, \dots, M$$

Where M is the number of time steps and Δt , is the size of a time step

$$\Delta t = \frac{t_{\max}}{M-1}$$

3.3.1 Finite Difference Approximations

The finite difference method involves using discrete approximations. i.e

$$\frac{\partial \phi}{\partial x} \approx \frac{\phi_{i+1} - \phi_i}{\Delta x}$$

Figure 3.1: is the mesh on a semi-infinite strip used for solution to the two-dimensional partial differential equation. The bold squares indicate the location of the initial values. The open squares indicate the location of the boundary values and the dots indicate the position of the interior points where the finite difference approximation is computed.

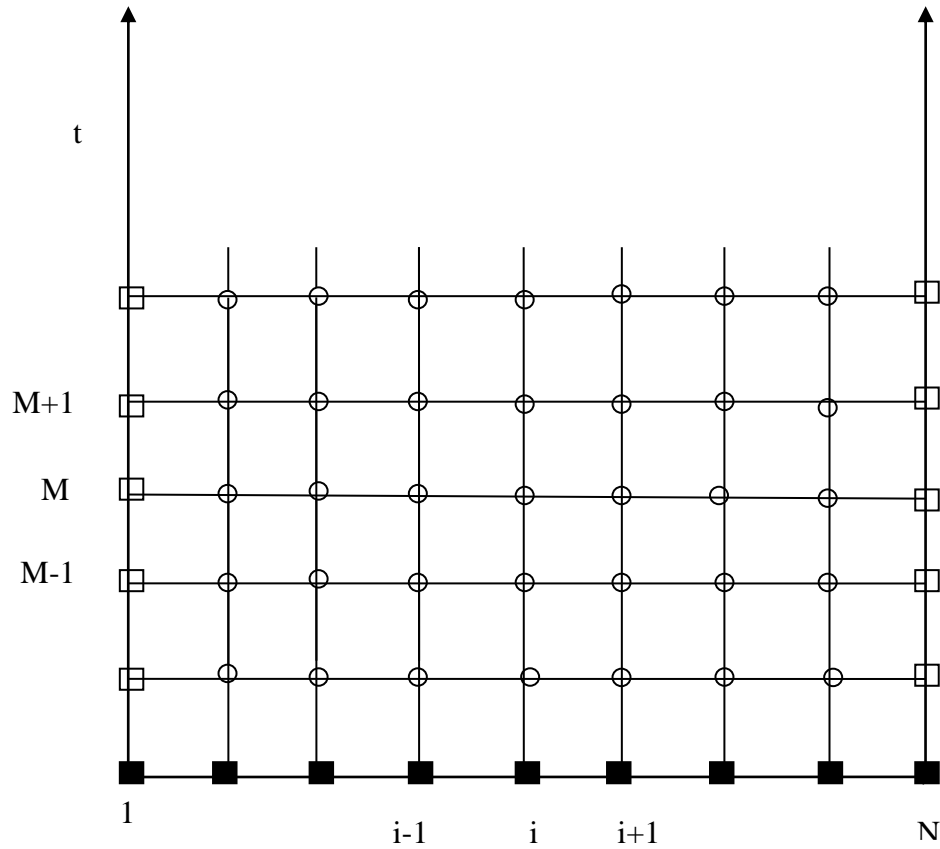


Figure 3.1: Finite difference mesh

3.3.2 First Order Forward Finite Difference

Consider a Taylor series expansion $\phi(x)$ about the point x_i

$$\phi(x_i + \partial x) = \phi(x_i) + \partial x \left. \frac{\partial \phi}{\partial x} \right|_{x_i} + \frac{\partial x^2}{2!} \left. \frac{\partial^2 \phi}{\partial x^2} \right|_{x_i} + \frac{\partial x^3}{3!} \left. \frac{\partial^3 \phi}{\partial x^3} \right|_{x_i} + \dots \quad (3.1)$$

Where ∂x is a change in x relative to x_i . Let $\partial x = \Delta x$ in Equation (3.1), i.e. consider the value of ϕ at the location of the x_{i+1} mesh line

$$\phi(x_i + \Delta x) = \phi(x_i) + \Delta x \left. \frac{\partial \phi}{\partial x} \right|_{x_i} + \frac{\Delta x^2}{2!} \left. \frac{\partial^2 \phi}{\partial x^2} \right|_{x_i} + \frac{\Delta x^3}{3!} \left. \frac{\partial^3 \phi}{\partial x^3} \right|_{x_i} + \dots \quad (3.2)$$

Solving for $\frac{\partial \phi}{\partial x} \Big|_{x_i}$

$$\frac{\partial \phi}{\partial x} \Big|_{x_i} = \frac{\phi(x_i + \Delta x) - \phi(x_i)}{\Delta x} - \frac{\Delta x}{2!} \frac{\partial^2 \phi}{\partial x^2} \Big|_{x_i} - \frac{\Delta x^2}{3!} \frac{\partial^3 \phi}{\partial x^3} \Big|_{x_i} + \dots \quad (3.3)$$

Substituting the approximate solution for the exact solution, i.e., use $\phi_i \approx \phi(x_i)$ and

$$\phi_{i+1} \approx \phi(x_i + \Delta x)$$

If the higher order derivatives are negligible then they can be given as

$$\frac{\Delta x^2}{2} \frac{\partial^2 \phi}{\partial x^2} \Big|_{x_i} + \frac{(\Delta x)^3}{3!} \frac{\partial^3 \phi}{\partial x^3} \Big|_{x_i} + \dots = \frac{\Delta x^2}{2} \frac{\partial^2 \phi}{\partial x^2} \Big|_{\xi} \quad (3.5)$$

where $x_i \leq \xi \leq x_{i+1}$. Thus

$$\frac{\partial \phi}{\partial x} \Big|_{x_i} \approx \frac{\phi_{i+1} - \phi_i}{\Delta x} + \frac{\Delta x^2}{2} \frac{\partial^2 \phi}{\partial x^2} \Big|_{\xi} \quad \text{or} \quad (3.6)$$

$$\frac{\partial \phi}{\partial x} \Big|_{x_i} - \frac{\phi_{i+1} - \phi_i}{\Delta x} \approx \frac{\Delta x^2}{2} \frac{\partial^2 \phi}{\partial x^2} \Big|_{\xi} \quad (3.7)$$

The term on the right hand side of Equation (3.7) is called the truncation error of the finite difference approximation. It is the error that results from truncating the series in Equation (3.4). In general, ξ is not known. Furthermore, since the function $\phi(x, t)$

is also unknown, $\frac{\partial^2 \phi}{\partial x^2}$ cannot be computed. Although the exact magnitude of the

truncation error cannot be known (unless the true solution $\phi(x, t)$ is available in analytical form), the “big O ” notation can be used to express the dependence of the truncation error on the mesh spacing. The right hand side of Equation (3.7) contains

the distance interval Δx , which is chosen by the person using the finite difference simulation. Since this is the only parameter under the user's control that determines the error, the truncation error is simply written

$$\frac{\Delta x^2}{2} \frac{\partial^2 \phi}{\partial x^2} \Big|_{\xi} = O(\Delta x^2) \quad (3.8)$$

The equals sign in this expression is true in the order of magnitude sense. In other words the “ $= O(\Delta x^2)$ ” on the right hand side of the expression is not a strict equality. Rather, the expression means that the left hand side is a product of an unknown constant and Δx^2 . Although the expression does not give us the exact magnitude of $\frac{\Delta x^2}{2} \frac{\partial^2 \phi}{\partial x^2} \Big|_{\xi}$, it tells us how quickly that term approaches zero as Δx is reduced.

Using big O notation, Equation (3.5) can be written

$$\frac{\partial \phi}{\partial x} \Big|_{x_i} = \frac{\phi_{i+1} - \phi_i}{\Delta x} + O(\Delta x) \quad (3.9)$$

Equation (3.9) is the forward difference formula for $\frac{\partial \phi}{\partial x} \Big|_{x_i}$ because it involves nodes x_i and x_{i+1} . The forward difference approximation has a truncation error that is $O(\Delta x)$. The size of the truncation error is under our control because we can choose the mesh size Δx . The part of the truncation error that is not under our control is $\partial^2 \phi / \partial x^2 \Big|_{\xi}$.

3.3.3 First Order Finite Central Difference

Taylor series expansions for ϕ_{i+1} and ϕ_{i-1} are

$$\phi_{i+1} = \phi_i + \Delta x \frac{\partial \phi}{\partial x} \Big|_{x_i} + \frac{\Delta x^2}{2} \frac{\partial^2 \phi}{\partial x^2} \Big|_{x_i} + \frac{(\Delta x)^3}{3!} \frac{\partial^3 \phi}{\partial x^3} \Big|_{x_i} + \dots \quad (3.10)$$

$$\phi_{i-1} = \phi_i - \Delta x \frac{\partial \phi}{\partial x} \Big|_{x_i} + \frac{\Delta x^2}{2} \frac{\partial^2 \phi}{\partial x^2} \Big|_{x_i} - \frac{(\Delta x)^3}{3!} \frac{\partial^3 \phi}{\partial x^3} \Big|_{x_i} + \dots \quad (3.11)$$

Subtracting Equation (3.11) from Equation (3.10) yields

$$\phi_{i+1} - \phi_{i-1} = 2\Delta x \frac{\partial \phi}{\partial x} \Big|_{x_i} + \frac{(\Delta x)^3}{3!} \frac{\partial^3 \phi}{\partial x^3} \Big|_{x_i} + \dots \quad (3.12)$$

Solving for $\frac{\partial \phi}{\partial x} \Big|_{x_i}$ gives

$$\frac{\partial \phi}{\partial x} \Big|_{x_i} = \frac{\phi_{i+1} - \phi_{i-1}}{2\Delta x} - \frac{(\Delta x)^3}{3!} \frac{\partial^3 \phi}{\partial x^3} \Big|_{x_i} + \dots \quad (3.13)$$

$$\frac{\partial \phi}{\partial x} \Big|_{x_i} = \frac{\phi_{i+1} - \phi_{i-1}}{2\Delta x} + o(\Delta x)^2 \dots \quad (3.14)$$

This is the central difference approximation to $\frac{\partial \phi}{\partial x} \Big|_{x_i}$. To get good approximations to

the continuous problem small Δx is chosen.

3.3.4 Second Order Finite Central Difference

Adding equation (3.11) and equation (3.10) yields

$$\phi_{i+1} + \phi_{i-1} = 2\phi_i + (\Delta x)^2 \frac{\partial^2 \phi}{\partial x^2} \Big|_{x_i} + \frac{2(\Delta x)^4}{4!} \frac{\partial^4 \phi}{\partial x^4} \Big|_{x_i} + \dots \quad (3.15)$$

Solving for $\frac{\partial^2 \phi}{\partial x^2} \Big|_{x_i}$ gives

$$\frac{\partial^2 \phi}{\partial x^2} \Big|_{x_i} = \frac{\phi_{i+1} - 2\phi_i + \phi_{i-1}}{(\Delta x)^2} + \frac{(\Delta x)^2}{12} \frac{\partial^4 \phi}{\partial x^4} \Big|_{x_i} + \dots \quad (3.16)$$

Or, using order notation,

$$\frac{\partial^2 \phi}{\partial x^2} \Big|_{x_i} = \frac{\phi_{i+1} - 2\phi_i + \phi_{i-1}}{\Delta x^2} + o(\Delta x)^2 \quad (3.17)$$

3.3.5 Crank-Nicholson method

The recommended method for most problems in the Crank-Nicholson algorithm, which has the virtues of being unconditionally stable and also is second order accurate in both the x and t directions (i.e., one can get a given level of accuracy with a coarser grid in the time direction, and hence less computation cost). The algorithm entails using difference expressions for the partial derivatives which are centered around $(t + k)/2$ rather than around t.

$$\frac{\partial^2 \mathbf{u}}{\partial x^2} = \frac{\mathbf{u}_{j+1,k} - 2\mathbf{u}_{j,k} + \mathbf{u}_{j-1,k} + \mathbf{u}_{j+1,k+1} - 2\mathbf{u}_{j,k+1} + \mathbf{u}_{j-1,k+1}}{2h^2} \quad (3.18)$$

3.4 Consistence, Convergence and Stability of a FDM

According to Mitchell (1980), the accuracy of a FDM is tested by using the following conditions which must be satisfied for a finite difference equation to be a reasonable approximate of the corresponding Partial Differential Equation.

3.4.1 Consistency

A finite difference equation (FDE) is said to be consistent if the difference between the Partial Differential Equation and its FDE vanishes or is negligible as the mesh is refined. That is the difference approaches zero.

3.4.2 Convergence

A finite difference equation is convergent if the solution of finite difference equation approaches the exact solution of the partial differential equation as the mesh sizes go to zero.

3.4.3 Stability

A finite difference method is said to be stable if the difference between the analytical and the numerical solutions of the difference equation remains bounded as time increases. That is the error does not propagate with time.

Using the following Finite differences

$$u = \frac{1}{2}(U_j^k + U_j^{k+1}) \quad (3.19)$$

$$\frac{\partial^2 u}{\partial r^2} = \frac{1}{2} \left(\frac{U_{j+1}^k - 2U_j^k + U_{j-1}^k}{(\Delta r)^2} + \frac{U_{j+1}^{k+1} - 2U_j^{k+1} + U_{j-1}^{k+1}}{(\Delta r)^2} \right) \quad (3.20)$$

$$\frac{\partial u}{\partial t} = \frac{U_j^{k+1} - U_j^k}{\Delta t} \quad (3.21)$$

$$\frac{\partial u}{\partial r} = \frac{1}{2} \left(\frac{U_j^k - U_{j-1}^k}{(\Delta r)} + \frac{U_j^{k+1} - U_{j-1}^{k+1}}{(\Delta r)} \right) \quad (3.22)$$

equation of momentum becomes:

$$\begin{aligned} \frac{U_j^{k+1} - U_j^k}{\Delta t} = \frac{\partial P}{\partial z} + \frac{1}{\text{Re}} \left(\frac{1}{2} \left(\frac{U_{j+1}^k - 2U_j^k + U_{j-1}^k}{(\Delta r)^2} + \frac{U_{j+1}^{k+1} - 2U_j^{k+1} + U_{j-1}^{k+1}}{(\Delta r)^2} \right) + \frac{1}{2r} \left(\frac{U_j^k - U_{j-1}^k}{(\Delta r)} + \frac{U_j^{k+1} - U_{j-1}^{k+1}}{(\Delta r)} \right) \right) \\ - M \frac{1}{2} (U_j^k + U_j^{k+1}) \end{aligned} \quad (3.23)$$

Making U_j^{k+1} the subject of the formula yields

$$\begin{aligned} U_j^{k+1} = \left(U_j^k + \Delta t \left(-\frac{\partial P}{\partial z} + \frac{1}{\text{Re}} \left(\frac{1}{2} \left(\frac{U_{j+1}^k - 2U_j^k + U_{j-1}^k + U_{j+1}^{k+1} + U_{j-1}^{k+1}}{(\Delta r)^2} \right) + \frac{1}{2r} \left(\frac{U_j^k - U_{j-1}^k - U_{j-1}^{k+1}}{(\Delta r)} \right) \right) - \frac{M}{2} U_j^k \right) \right) / \\ \left(1 + \frac{\Delta t}{\text{Re}(\Delta r)^2} + \frac{\Delta t}{2r \text{Re}(\Delta r)} + \frac{M\Delta t}{2} \right) \end{aligned} \quad (3.24)$$

Also using the following Finite differences

$$\frac{\partial T}{\partial t} = \frac{T_j^{k+1} - T_j^k}{\Delta t} \quad (3.25)$$

$$\frac{\partial T}{\partial r} = \frac{1}{2} \left(\frac{T_j^k - T_{j-1}^k}{\Delta r} + \frac{T_j^{k+1} - T_{j-1}^{k+1}}{\Delta r} \right) \quad (3.26)$$

$$\frac{\partial^2 T}{\partial r^2} = \frac{1}{2} \left(\frac{T_{j+1}^k - 2T_j^k + T_{j-1}^k}{(\Delta r)^2} + \frac{T_{j+1}^{k+1} - 2T_j^{k+1} + T_{j-1}^{k+1}}{(\Delta r)^2} \right) \quad (3.27)$$

$$\frac{\partial u}{\partial r} = \frac{1}{2} \left(\frac{U_j^k - U_{j-1}^k}{\Delta r} + \frac{U_j^{k+1} - U_{j-1}^{k+1}}{\Delta r} \right) \quad (3.28)$$

Equation of energy becomes

$$\begin{aligned} \frac{u_0 a_0}{\mu} \frac{T_j^{k+1} - T_j^k}{\Delta t} &= \frac{1}{\mu \text{Pr}} \left(\frac{1}{2} \left(\frac{T_{j+1}^k - 2T_j^k + T_{j-1}^k}{(\Delta r)^2} + \frac{T_{j+1}^{k+1} - 2T_j^{k+1} + T_{j-1}^{k+1}}{(\Delta r)^2} \right) + \frac{1}{2} \left(\frac{T_j^k - T_{j-1}^k}{\Delta r} + \frac{T_j^{k+1} - T_{j-1}^{k+1}}{\Delta r} \right) \right) + \\ \frac{Ec}{\rho} \left(\frac{1}{2} \left(\frac{U_j^k - U_{j-1}^k}{\Delta r} + \frac{U_j^{k+1} - U_{j-1}^{k+1}}{\Delta r} \right) \right)^2 &+ \left(\frac{H}{(T_w - T_\infty)} \frac{U_j^k + U_j^{k+1}}{2} \right) \end{aligned} \quad (3.29)$$

Making T_j^{k+1} the subject of the formula yields

$$\begin{aligned} T_j^{k+1} &= \left(T_j^k + \frac{\mu \Delta t}{u_0 a_0} \left(\frac{\text{Pr}}{\mu} \left(\frac{T_{j+1}^k - 2T_j^k + T_{j-1}^k + T_{j+1}^{k+1} + T_{j-1}^{k+1}}{2(\Delta r)^2} \right) + \left(\frac{T_j^k - T_{j-1}^k - T_{j-1}^{k+1}}{2\Delta r} \right) \right) + \frac{Ec}{\rho} \left(\frac{U_j^k - U_{j-1}^k + U_j^{k+1} - U_{j-1}^{k+1}}{2(\Delta r)} \right) + \frac{H}{T_w - T_\infty} \left(\frac{U_j^k + U_j^{k+1}}{2} \right) \right) / \\ \left(1 + \frac{\Delta t \text{Pr}}{u_0 a_0 (\Delta r)^2} - \frac{\Delta t \text{Pr}}{2u_0 a_0 \Delta r} \right) & \end{aligned} \quad (3.30)$$

In the next chapter the obtained final finite difference equations (3.24) and (3.30) are implemented in matlab and the results are represented in form of graphs and discussed.

CHAPTER FOUR

RESULTS AND DISCUSSIONS

4.1 Introduction

In this chapter, we present the results followed by discussions. The solutions are obtained by first converting the partial differential equations into algebraic equations .MATLAB is then used to output the results.

Equations (3.24) and (3.30) were solved using the MATLAB version 7.9.0.529(R2009b). computer code in Appendix I. Computations for the primary velocity u and temperature T were made for various parameters .The parameters that were varied include Reynolds number pressure gradient, magnetic parameter, Eckert number , Prandtl number, Hartman number and time. The reference values represented in the figures are $Re=7.1, \frac{\partial P}{\partial z} = -10, M=4, Ec=0.5, Pr=21$ and $H=4$. These parameters were varied one at a time and input into a computer program. Computations were done using equations (3.23) and (3.29), the initial conditions $u=0, T=0$ and the boundary conditions $u=0.45, T=37$ for $r=0$ and $u=0, T=0$ for $r=1$ and the curves were plotted for each case. These results were then represented in the figures labeled Figure (4.1) on page (35) to Figure (4.7) on page (41).

4.2 Primary velocity profiles

A glimpse on the outlook of the numerical solutions for velocity is provided below.

GRAPH OF THE VELOCITY VERSUS RADIAL DISTANCE OF THE COLLAPSIBLE TUBE WITH REYNOLDS NUMBER CHANGING

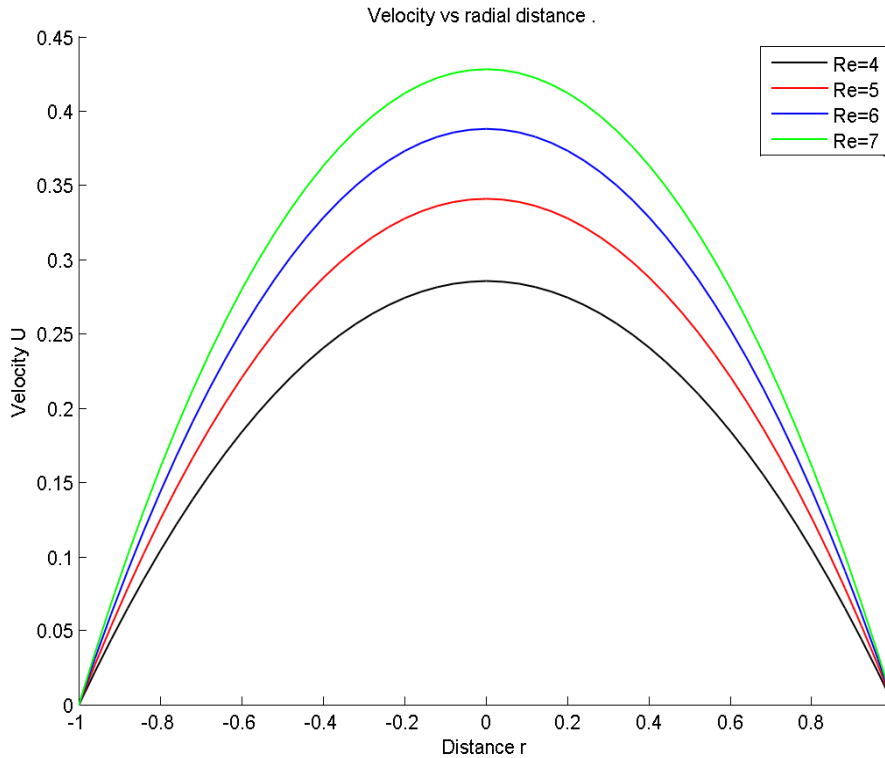


Figure 4.1: Velocity profiles for $M=4$, $P= -10$, $t=100$

From Figure 4.1 it is observed that when the Reynolds number is increased holding M and P constants the magnitude of the primary velocity profiles increased with maximum value at the center. This can be explained by, as the Reynolds number increase the viscous forces decrease .As these viscous forces which oppose the motion of the fluid decrease the velocity of the fluid increase.

GRAPH OF THE VELOCITY VERSUS RADIAL DISTANCE OF THE COLLAPSIBLE TUBE WITH MAGNETIC PARAMETER CHANGING

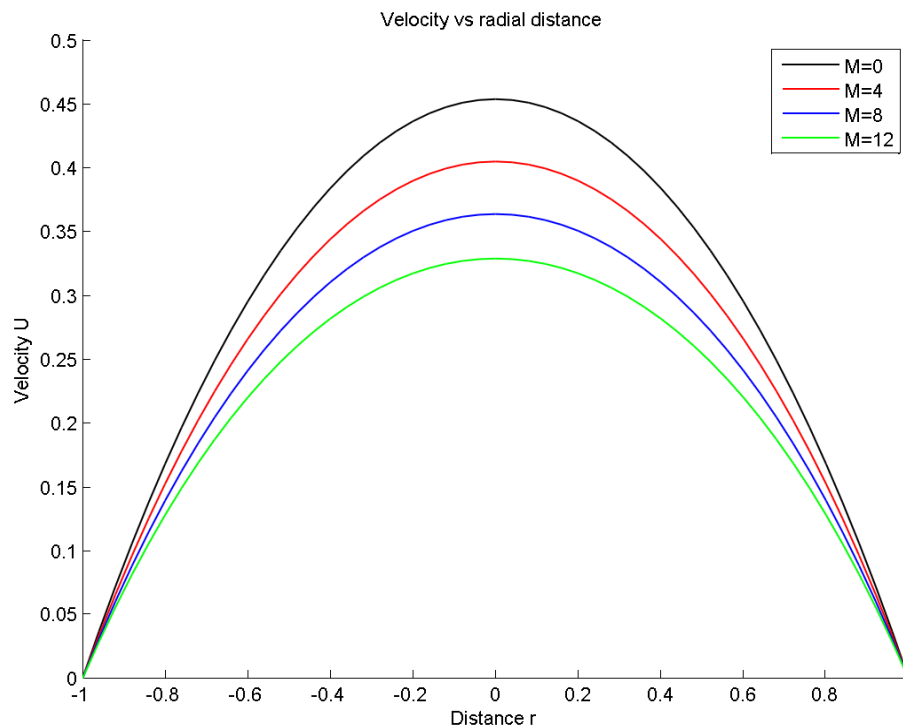


Figure 2.2: Velocity profiles for $Re=7.1$, $P=-10$, $t=100$

From Figure 4.2 it is observed that when the magnetic parameter is increased holding Re and P constants the magnitude of the primary velocity profiles decreased. This is because Introduction of strong magnetic field normal to the direction of electrically conducting fluid results to emergence of a resistive force to the main flow. This resistive force called Lorentz force resists the flow of the fluid resulting to deceleration of the fluid and thus the fluid velocity profiles reduces.

GRAPH OF THE VELOCITY VERSUS RADIAL DISTANCE OF THE COLLAPSIBLE TUBE WITH TIME CHANGING

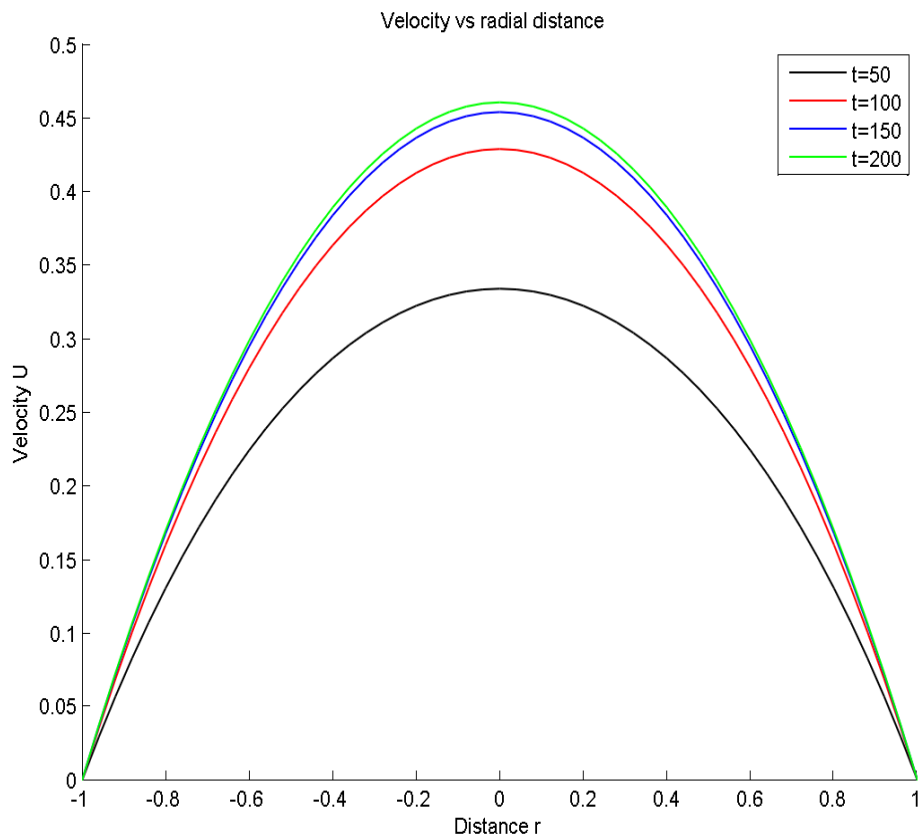


Figure 4.3: Velocity profiles for $Re=7.1$, $M=4$, $P=-10$

From Figure 4.3 it is observed that when time is increased holding Reynolds number and magnetic parameter constants the primary velocity profiles increased. This is because with time the flow gets to the free stream and therefore its velocity increases.

GRAPH OF THE VELOCITY VERSUS RADIAL DISTANCE OF THE COLLAPSIBLE TUBE WITH PRESSURE GRADIENT CHANGING

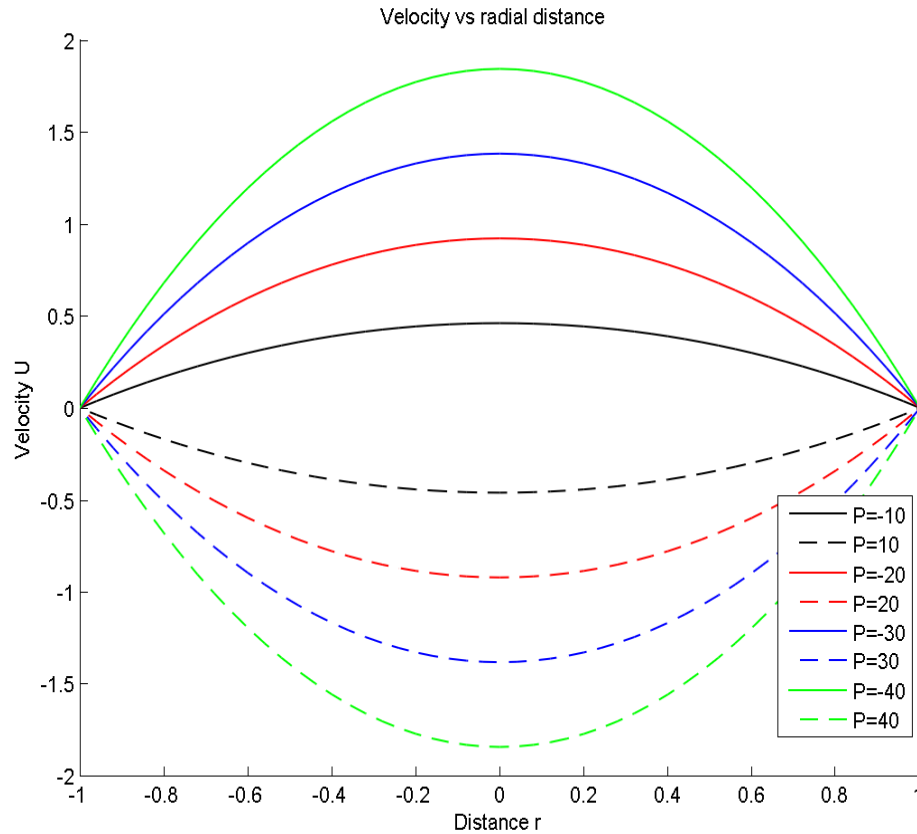


Figure 4.4: Velocity profiles for $Re=7.1$, $M=4$, $t=100$

From Figure 4.4 it is observed that when the pressure gradient is negative it leads to an increase in the primary velocity profiles in the positive direction. When the pressure gradient is positive it leads to an increase in the primary velocity profiles in the negative direction. This is because when pressure gradient is positive, then the pressure force term acts in the opposite direction of the direction of the fluid flow. On the other hand, when it is negative, then the pressure force term acts in the same direction as that of the fluid flow hence aiding the fluid flow.

4.3 Temperature profiles

A glimpse on the outlook of the numerical solutions for temperature is provided below.

GRAPH OF THE TEMPERATURE VERSUS RADIAL DISTANCE OF THE COLLAPSIBLE TUBE WITH PRANDTL NUMBER CHANGING

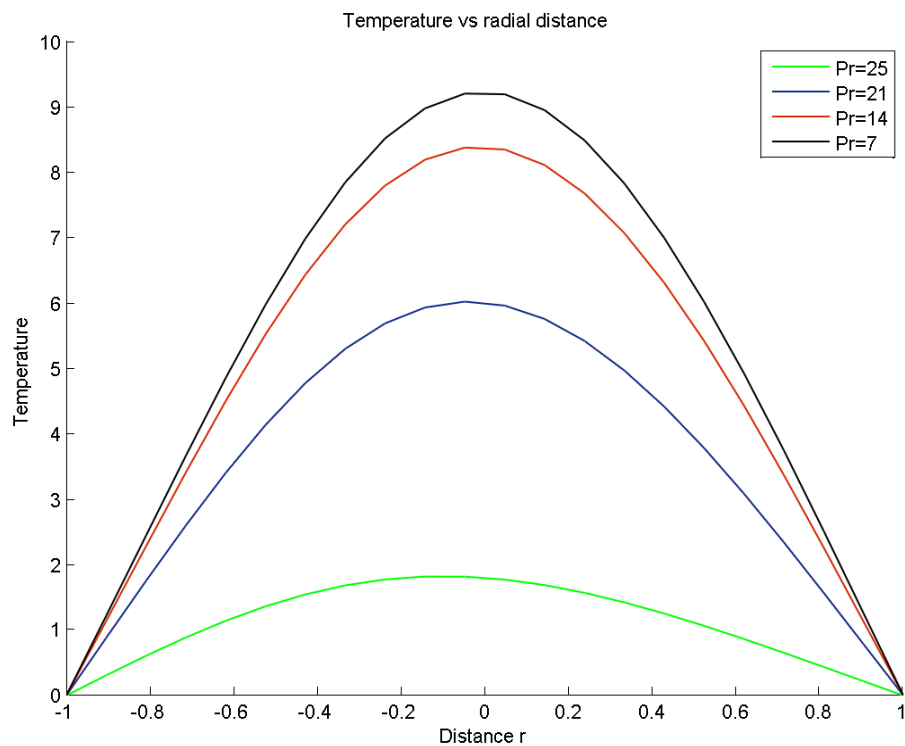


Figure 4.5: Temperature profiles for $H=4$, $Ec=0.5$, $t=100$

From Figure 4.5 it is observed that when Prandtl number was increased holding Eckert number and Hartmann number constant the temperature profiles decreased. A rise in Prandtl number leads to a decrease in temperature distribution because an increase in Prandtl number means a slow rate in thermal diffusion.

GRAPH OF THE TEMPERATURE VERSUS RADIAL DISTANCE OF THE COLLAPSIBLE TUBE WITH ECKERT NUMBER CHANGING

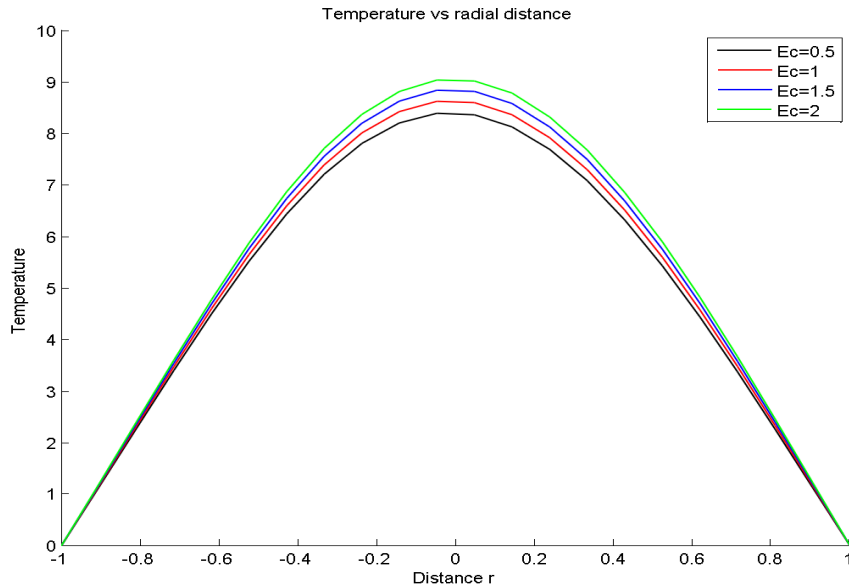


Figure4.6: Temperature profiles for $H=4, Pr=21, t=100$

From Figure 4.6 it is observed that when Eckert number was increased holding Prandtl number and Hartmann number constant the temperature profiles increased. The temperature profile is parabolic with maximum temperature at the center of the collapsible tube. This result shows that as the Eckert number is increased, the rate at which fluid loses heat decreases and hence there will be an increase in the temperature of the fluid. This behavior is attributed to the decrease of viscous dissipation as Eckert increases. Increase in Eckert number reduces the temperature gradient thus increasing the temperature boundary layer and therefore the increase in temperature. Increased kinetic energy when the fluid absorbs more heat energy that is released from the internal viscous forces leads to Increase in Eckert number. This

heat increases the temperature of the fluid which is depicted by increase in temperature profiles.

GRAPH OF THE TEMPERATURE VERSUS RADIAL DISTANCE OF THE COLLAPSIBLE TUBE WITH HARTMANN NUMBER CHANGING

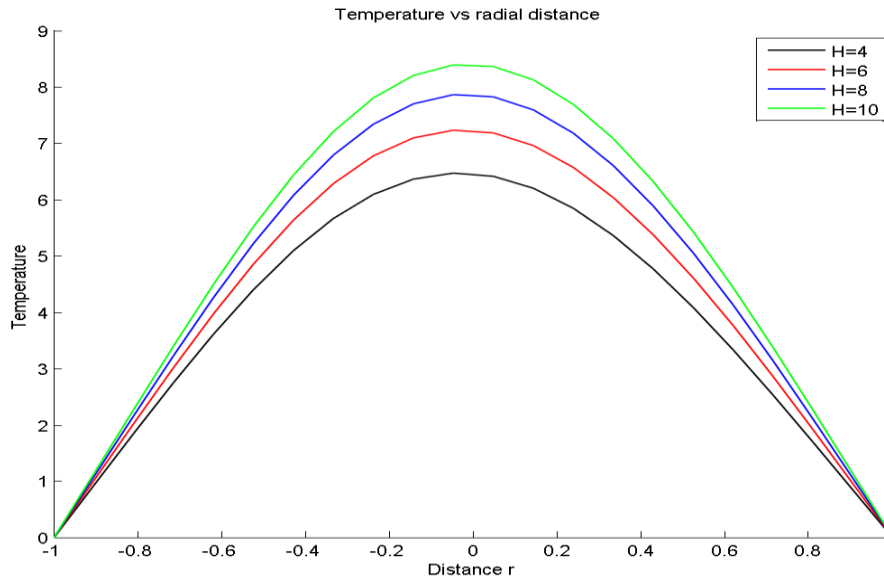


Figure4.7: Temperature profiles for $Pr=21$, $Ec=0.5$, $t=100$

From Figure 4.7 it is observed that when Hartmann number was increased holding Prandtl number and Eckert number constant the temperature profiles increased. The rise in temperature is as a result of interaction between the atomic ions that constitute conductor and the moving particles that form the current. The charged particles in the electric circuit are speeded up by the electric field but they lose some kinetic energy whenever they collide with ions. The increase in vibration energy of the ions manifests itself as heat that is depicted by the rise of temperature of the fluid. The increased fluid temperature results to non- uniform changes in fluid properties like fluid density and conductivity. Thus energy is converted from electrical power supply to the fluid or any other medium that is in thermal contact. This heat is referred to as joules heating.

4.4 Validation of Results

From this research unsteady magnetohydrodynamic fluid flow in a collapsible tube has been investigated. It is found that an increase in magnetic parameter leads to a decrease in velocity of the fluid. When magnetic field is not considered in the flow the results are similar to those of Odejide (2008) who found that an increase in Reynolds number lead to an increase in the velocity of the fluid.

The conclusions of this research study have been done in the next chapter. Finally, recommendations of areas on collapsible tubes that require further research have also been outlined.

CHAPTER FIVE

CONCLUSIONS AND RECOMMENDATIONS

5.1 Introduction

In this chapter conclusions of the research carried out are outlined and thereafter recommendations for future research work were also made.

5.2 Conclusions

This study involved unsteady magnetohydrodynamic fluid flow in a collapsible tube. The objectives of this study were to determine the velocity profiles, temperature profiles and to determine the effects of varying some selected dimensionless numbers on the flow parameters. Equations governing the fluid flow that are developed are momentum equation and energy equation. A non-dimensionalisation scheme was used to non-dimensionalize the governing equations. A finite difference scheme was used to write the equations in finite difference form. A computer program was written and run to generate velocity and temperature profiles and presented in graphical form as depicted in chapter three.

The following conclusions on the effects of each non-dimensional parameter were made;

- i. Increase in Reynolds number leads to an increase in magnitude of the primary velocity of the flow
- ii. Increase in magnetic parameter leads to a decrease in magnitude of the primary velocity of the flow
- iii. Increase in time increases both the velocity profiles and temperature profiles.
- iv. An increase in Prandtl number causes a decrease in temperature profiles.
- v. Increase in the Eckert number causes increase in temperature profiles.

- vi. Increase Hartmann number results to an increase in temperature profiles.

From these conclusions the objectives of the study were achieved.

5.3 Recommendations

This study considered unsteady magnetohydrodynamic fluid flow in a collapsible tube. The study on MHD flows in collapsible tubes have a wide area of study. Most of it was not considered in this thesis and can be investigated in future because of its importance in its applications in Medicine and Engineering.

Some of the areas that can be researched on in future include:

- i. Fluid flow through collapsible tube for a turbulent flow.
- ii. Flow through collapsible tube with tensile force varying
- iii. Flow through other geometric shapes of collapsible tube.
- iv. Flow through porous collapsible tube.
- v. Compressible fluid flow through a collapsible tube.

REFERENCES

- Andrew, I. and Matthias, H. (2003), Steady finite-Reynolds-number flows in three-dimensional collapsible tubes, *Journal of Fluid Mechanics*, 486, 79-103.
- Bertram, C.D. (1986). Unstable equilibrium behavior in collapsible tubes, *Biomechanical Journal*, 19(1), 61-69.
- Bertram, C.D., Raymond, C.J. and Pedley, T.J., (1990), Mapping of instabilities for flow through collapsible tubes of differing lengths, *Journal of Fluid structures*, 4(2), 125-153.
- Boileau, E. (2015). A benchmark study of numerical schemes for one-dimensional arterial blood flow modeling, *International Journal for Numerical Methods in Biomedical Engineering*, 31(10).
- Brian, D.T. (2003). *Computational methods for flow in collapsible tubes*, MSc, Texas Tech University, Texas, USA. 13, 279–290.
- Annunziato, S. (2013). Flow in Collapsible tubes with Discontinuous mechanical properties: Mathematical model and exact solutions, *Communications in Computational Physics Journal*, 13(2), 361-385.
- Emilie, M. and Patrice, F. (2010), Accurate modeling of unsteady flows in collapsible tubes, *Computer Methods in Biomechanics and Biomedical Engineering*, 13(2), 279–290.
- Hazel, A. and Heil, M. (2003), Steady finite-Reynolds number flows in three dimensional collapsible tubes, *Journal of fluid Mechanics*, 486, 79-103.
- Jensen, O.E., Heil, M., (2003), High frequency self-excited oscillations in a collapsible channel flow, *Journal of Fluid Mechanics*, 481, 235-268.
- Kanyiri, C. Kinyanjui, M.N. and Kang’ethe, G. (2014). Effects of flow parameters on flow variables of a Newtonian fluid through a cylindrical collapsible tube. *Mathematical Theory and Modeling*, 4, 7-17.
- Liu, H.F., Luo, X.Y., Cai, Z.X. and Pedley, T.J. (2009), Sensitivity of unsteady collapsible channel flows to modeling assumptions, *Communications in Numerical Methods in Engineering*, 25(5), 483-504.
- Makinde, O. D. (2005). Collapsible Tube Flow: A Mathematical Model, *Romanian Journal of Physics*, 50(5/6), 493-506.

- Marzo, A., Luo, X.Y. and Bertram, C.D. (2005), Three-dimensional collapse and steady flow in thick-walled flexible tubes, *Journal of Fluids and Structures*, 20(6), 817–835.
- Mawasha, P.R., Ted, A.C. and Paul, C. L. (2001), Investigations of dynamic behavior of a collapsible tube model through nonlinear analysis, *Cardiovascular Engineering, An International Journal*, 1(14), 183-189.
- Odejide, S.A., Aregbesola, Y.A. and Makinde, O. D. (2008), Fluid Flow and Heat Transfer in a Collapsible Tube, *Romanian Journal of Physics*, 53, 499–506.
- Prashanta, K.N. (2005). An unsteady analysis of non-Newtonian blood flow through tapered arteries with a stenosis, *International journal of Non-linear mechanics*, 40(1), 151-164.
- Siviglia, A. and Toffolon, M, (2013) Steady analysis of transcritical flows in collapsible tubes with discontinuous mechanical properties: implications for arteries and veins, *J. Fluid Mech*, 736, 195-215.

APPENDICES

COMPUTER CODE IN MATLAB

In order to solve the governing equations (3.16) and (3.18), the following computer program code was developed using matlab software version 7.9.0 (R2009b), subject to the boundary conditions as discussed herein. The results were obtained by varying various flow parameters.

% NUMERICAL SOLUTION OF FLOW IN COLLAPSIBLE TUBE

```
function newlyimproved2()
clear all;
clc;
Re=7;M=5;a0=0.3;alpha=0.2347;P=-
10;neu=0.00305;Pr=20;U0=1;Ec=0.05;H=100;
Q=2;rho=1025;Cp=3400;
Tw=0;Tinf=-310;tp=600;ttp=500;
nz=21;nr=21;nt=1000;
delt=0.001;
delr=0.05;
X=linspace(-1,1,nr+1);
U=zeros(nr,nt);
T=zeros(nr,nt);

% initial conditions
for i=1:nz+1
    for j=1:nr+1
        for k=1:nt+1
            U(j,1)=0;
            T(j,1)=0;
        end
    end
end
% boundary condtions
for i=1:nz+1
    for k=1:nt+1
        for j=1:nr+1
            U(1,k)=0;
            T(1,k)=0;
        end
    end
end
for i=1:nz+1
    for k=1:nt+1
        for j=1:nr+1
            U(11,k)=1;
            T(11,k)=37;
        end
    end
end
for i=1:nz+1
    for k=1:nt+1
        for j=1:nr+1
```

```

    U(nr+1,k)=0;
    T(nr+1,k)=0;
    end
end
end

for k=1:nt
    for i=2:nz
        for j=2:nr
            r=a0*((1-(alpha*(k-1)))^0.5);

U(j,k+1)=(U(j,k)+delt*(-P+(1/Re)*((U(j+1,k)-2*U(j,k)+U(j-1,k)+U(j+1,k+1)+U(j-1,k+1))/(2*delr^2))+((U(j,k)-U(j-1,k)-U(j-1,k+1))/...*(2*r*delr)))-((M/2)*U(j,k)))/(1+(delt/(Re*delr^2))-(delt/(2*r*Re*delr))+((M*delt)/2));

T(j,k+1)=(T(j,k)+((neu*delt)/(U0*a0))*(((1/Pr)*neu)*((T(j+1,k)-(2*T(j,k))+T(j-1,k)+T(j+1,k+1)+T(j-1,k+1))/(2*delr^2))+((T(j,k)-T(j-1,k)-T(j-1,k+1))/(2*r*delr)))+(Ec/rho)*((U(j,k)-U(j-1,k)+U(j,k+1)-U(j-1,k+1))/(2*delr))^2))+((H/(TwTinf))*((U(j,k)+U(j,k+1))/(2)))+(Q*a0^2)/(neu*rho*Cp*(Tw-Tinf))))/(1+((delt*(1/Pr))/(U0*a0*delr^2))*((delt*(1/Pr))/(2*U0*a0*r*delr)));

            end
        end
    end
    figure(1)
    hold on
    grid off
    plot(X,U(:,tp),'g','LineWidth',1,'LineSmoothing','on');
    title('Velocity vs Distance along the plate.');
```

xlabel('Distance x');
 ylabel('Velocity U');
 hold off

```

    figure(2)
    hold on
    grid off
    plot(X,T(:,ttp),'g','LineWidth',1,'LineSmoothing','on');
    title('Temperature vs Distance along the plate.');
```

xlabel('Distance x');
 ylabel('Temperature');
 hold off

PUBLICATION

J.M. Kigo, M.N. Kinyanjui, K.Giterere, P.R.Kiogora (2015) Unsteady Magneto hydrodynamic fluid flow in a collapsible tube. *International Journal of science and innovative Technology* 4,111-118